



## Role of chlorine on the opto-electronic properties of $\beta$ - $\text{In}_2\text{S}_3$ thin films

Angel Susan Cherian<sup>\*</sup>, Meril Mathew, C. Sudha Kartha, K.P. Vijayakumar

Department of Physics, Cochin University of Science and Technology, Kochi 682022, India

### ARTICLE INFO

Available online 20 September 2009

#### Keywords:

$\beta$ - $\text{In}_2\text{S}_3$   
Spray pyrolysis  
Chlorine doping

### ABSTRACT

Effect of chlorine doping on the opto-electronic properties of  $\beta$ - $\text{In}_2\text{S}_3$  thin film, deposited by spray pyrolysis technique is studied for the first time. Chlorine was incorporated in the spray solution, using HCl. Pristine sample prepared using  $\text{In}(\text{NO}_3)_3$  and thiourea as the precursors showed very low photosensitivity. But upon adding optimum quantity of chlorine, the photosensitivity increased by 3 orders. X-ray analysis revealed that crystallinity was also increasing up to this optimum level of Cl concentration. It was also observed that samples with high photosensitivity were having higher band gap. The present study proved that doping with chlorine was beneficial as this could result in forming crystalline and photosensitive films of indium sulfide.

© 2009 Elsevier B.V. All rights reserved.

### 1. Introduction

It is well accepted that an efficient thin film solar cell, prepared using a simple technique, could be the solution to reduce the high cost in the present fabrication process of solar cells. Research groups worldwide are working on the metal chalcogenide materials [1] especially those which can be prepared using soft techniques like spray pyrolysis [2] and chemical bath deposition [3]. Among them, the III–VI semiconductor,  $\text{In}_2\text{S}_3$  has been the centre of attraction during the past two decades, primarily due to its opto-electronic properties and its potential use in the fabrication of semiconductor devices. Replacement of a divalent metal in II–VI compound, ZnS by one of the trivalent ones like indium leads to the formation of  $\text{In}_2\text{S}_3$  having a defect structure. In this material, the sulfur atoms form a cubic or hexagonal close packed structure and a part of cation sites remain empty [4,5]. Because of its high defect structure, this material finds several application in the preparation of red and green phosphors for television picture tubes [6], dry cells [7] and photochemical cells [8] etc. With optimal physical properties, this semiconductor material can meet the requirements of window material or buffer layer in solar cells [9,21,22].

The important aim of research efforts on this material is the replacement of compounds having toxic and heavy metals. Replacement of *n*-type CdS layer in polycrystalline heterojunction thin film solar cells is of particular interest.  $\text{Cu}(\text{In,Ga})\text{Se}_2$  based solar cell, prepared with chemical bath deposited  $\text{In}_2\text{S}_3$  as the buffer layer, could reach efficiencies (15.7%) near to that of a standard cell with CdS buffer layer [10]. Our group obtained an efficiency of 9.5% for a  $\text{CuInS}_2/\text{In}_2\text{S}_3$  thin film solar cell prepared using the spray pyrolysis technique

[11]. Moreover  $\text{In}_2\text{S}_3$  has a wider band gap, which can reduce the optical transmission loss at short wavelengths occurring in the CdS [12]. Hence development of this eco-friendly material is essential for large scale terrestrial applications.

Indium sulfide is an *n*-type semiconductor by birth, existing in three forms; a defect cubic  $\beta$ -structure under ambient conditions; a defect spinel  $\beta$ - $\text{In}_2\text{S}_3$  formed at 693 K; and  $\beta$ - $\text{In}_2\text{S}_3$  formed at 1013 K [13–15]. Among these,  $\beta$ - $\text{In}_2\text{S}_3$  is the stable phase of  $\text{In}_2\text{S}_3$  from room temperature to 693 K and it crystallizes in a defect spinel lattice with a high degree of vacancies, ordering at tetrahedral cation sites [16]. The unit cell of this superstructure, exhibiting tetragonal symmetry, consists of three spinel cubes, stacked along the *c*-axis. In the spinel type structure, all the octahedral sites are occupied by indium atoms. But in the 12 tetrahedral sites, normally 4 sites are remaining empty. Thus 33% of the indium sites are remaining vacant i.e. neighboring sulfur atoms are bonded only to three instead of the usual four indium atoms and these vacant sites will exhibit electron affinity, acting as electron traps. This ordered modification can be interpreted as a quasi-ternary compound consisting of In, S and vacancies [17]. A small fraction of In atoms may leave their ordered positions and occupy crystallographically ordered vacancies [18]. This results in a number of quasi-interstitial cations and an equal number of cation vacancies, so that in a stoichiometric crystal of  $\beta$ - $\text{In}_2\text{S}_3$ , a considerable degree of disorder is always present. The small fractions of disordered cations and cation vacancies act as donors and acceptors, nearly compensating each other. In the case of disordered vacancies, the crystal would retain its cubic symmetry and if the vacancies are ordered, the crystal symmetry would be lowered [19]. Defect levels in  $\beta$ - $\text{In}_2\text{S}_3$  have been assigned using PL and TSC studies by our group [12].

Among a number of techniques that can be used to prepare thin film materials, chemical spray pyrolysis [CSP] is a technique that meets the requirements, involved in the manufacturing process for solar cell devices. Spray pyrolysis has been chosen by several researchers [20] due

<sup>\*</sup> Corresponding author.

E-mail address: [angelsusanc@yahoo.com](mailto:angelsusanc@yahoo.com) (A.S. Cherian).

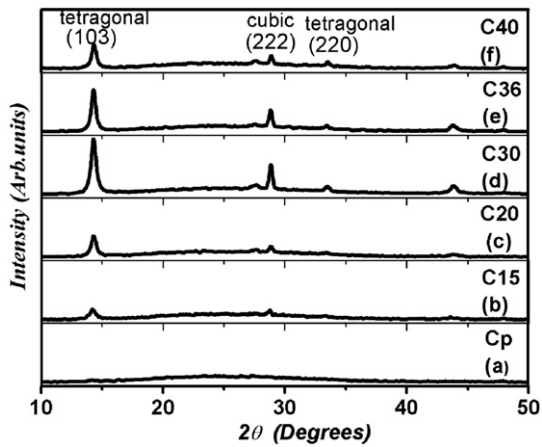


Fig. 1. XRD plots of pristine and Cl doped samples.

to its simplicity and versatility to prepare semiconductor materials. By controlling the deposition parameters using spray pyrolysis,  $\text{In}_2\text{S}_3$  thin films could be produced with optimized opto-electronic properties.

Interestingly, only very few investigations have reported on doping of  $\text{In}_2\text{S}_3$  films, so as to modify its structural and electrical properties. Becker et al. reported that doping of  $\text{In}_2\text{S}_3$  films with Sn resulted in samples with low resistance [23]. Kim et al. reported that doping of indium sulfide single crystals with cobalt, leads to the decrease of the structural defects [24]. N. Kamoun et al. reported that the presence of Al caused an increase in adsorption of oxygen in the sample [25]. Roland Diehl and Rudolf Nitsche [15], reported stabilization of  $\gamma\text{-In}_2\text{S}_3$ , (which is the high temperature phase of  $\text{In}_2\text{S}_3$ ) at room temperature by replacing about 5 to 10% of In atoms by As, Sb or Bi. Barreau et al. reported that incorporation of Na resulted in wider band gap and better conductivity [17]. Recently we reported that Ag doping resulted in samples with enhanced crystallinity, conductivity and photosensitivity [18]. Chlorine doping was identified as a very efficient compensation mechanism for obtaining highly resistive polycrystalline CdTe for solar cell application [27].

The primary aim of the present work is to study the role of chlorine doping on  $\beta\text{-In}_2\text{S}_3$  thin films. Most of the research work on  $\text{In}_2\text{S}_3$  prepared by CSP has been carried out using  $\text{InCl}_3$  and thiourea as precursor solutions. The samples prepared using chloride based precursors were highly crystalline and photosensitive [20]. But the samples prepared using nitrate based precursors ( $\text{In}(\text{NO}_3)_3$  and thiourea) were amorphous and less photosensitive [26]. Hence it was strongly suspected that the high photosensitivity and crystallinity of chloride based samples might be due to the effect of chlorine on  $\beta\text{-In}_2\text{S}_3$  films. In the present paper, we depict the effect of Cl doping on structural, electrical, and optical properties of spray pyrolyzed  $\beta\text{-In}_2\text{S}_3$  thin films by purposefully adding Cl to the solution of Indium nitrate and Thiourea.

## 2. Experimental details

$\text{In}_2\text{S}_3$  thin films were deposited on soda lime glass substrates using chemical spray pyrolysis (CSP) technique and the experimental details

**Table 1**  
Grain size calculated for  $2\theta = 14.3^\circ$ .

Sample	Grain size
C15	15.67 nm
C20	19.76 nm
C30	21.35 nm
C36	26.59 nm
C40	23.60 nm

were reported elsewhere [20,26]. The spraying solution contained  $\text{In}(\text{NO}_3)_3$  and  $\text{CS}(\text{NH}_2)_2$  maintaining a ratio between In and S at 2:8. This ratio was selected as in the samples prepared using this solution, sulfur has gained a stoichiometric composition of 60% with oxygen only as a surface contaminant and also granularity of samples is regained at this ratio [26]. 200 ml of the solution was sprayed onto the glass substrate, kept at a temperature of  $573 \pm 5$  K, at a spray rate of 20 ml/min. Thickness of the film was 0.2  $\mu\text{m}$ . In order to dope these samples with chlorine, different volumes of 0.5 M HCl (10 ml, 20 ml, 30 ml, 36 ml and 40 ml) were added to the solution. The doped samples were named as C10, C20, C30, C36 and C40 respectively and the pristine sample was named as Cp.

Structural properties of pristine and doped films were determined by means of X-ray diffraction (XRD) (Rigaku-D, Max.C-X-ray diffractometer having  $\text{Cu K}\alpha$  radiation of wavelength, 1.5405 Å). Morphological studies were done with the help of scanning electron microscope (SEM) (Cambridge model). Atomic concentrations of the elements present in the samples were determined using energy dispersive X-ray analysis (EDAX) (Oxford model 7060). X-ray photoelectron spectroscopy (XPS), (ULVAC-PHI unit, model: ESCA 5600 CIM capable of employing argon ion sputtering), was used to obtain the depth profile and atomic ratio of the films. Optical properties were obtained from optical absorption spectra (UV-VIS-IR spectrophotometer-JASCO V-570 model). Photoluminescence (PL) measurements were carried out at room temperature using He-Cd laser, having wavelength of 325 nm, which lies in the above band gap region and hence the excitation is called above band gap excitation (intrinsic excitation). Emission spectra were analyzed by employing spectrophotometer (Ocean Optics USB2000), having a Si charge coupled device (CCD) array detector. Photosensitivity  $\{I_L - I_D\}/I_D$ , where  $I_L$  is the illuminated current and  $I_D$  is the dark current) measurements were performed using Keithley 236 source measure unit. For the photocurrent measurement, the sample was illuminated with a tungsten halogen lamp (60  $\text{mW}/\text{cm}^2$ ). Electrical contacts were made using silver paint, in the form of two end contacts, having a distance of 5 mm between them.

## 3. Results and discussions

### 3.1. Structure and morphology

#### 3.1.1. XRD Analysis

Fig. 1(a) shows the XRD pattern of pristine  $\text{In}_2\text{S}_3$  thin film and Fig. 1(b)–(f) depicts the XRD patterns of chlorine doped  $\text{In}_2\text{S}_3$  samples. Pristine  $\text{In}_2\text{S}_3$  film prepared using  $\text{In}(\text{NO}_3)_3$  was almost amorphous. But with chlorine doping, crystallinity of the films improved. However, it was also evident that there was an optimum value of doping, up to which the crystallinity increased and after that a retracing phenomenon was observed. The  $d$  values coincided with that of the  $\beta\text{-In}_2\text{S}_3$  in standard JCPDS data card (25-390). The samples showed  $\beta\text{-In}_2\text{S}_3$  phase with an orientation along the (103) plane at  $2\theta = 14.3$ . Here the intensity of Bragg peaks in XRD pattern increased up to the sample C30 and started decreasing when chlorine concentration was increased further. Grain size calculated using Debye-Scherrer formula [20] also showed a considerable increase with chlorine doping (Table 1). The grain size increased from 15.6 nm to 26.6 nm with Cl doping and then it started decreasing for the sample N40. XRD studies indicated the

**Table 2**  
Atomic concentration of elements from EDAX analysis.

Sample	In%	S%	Cl%	In/S%
Cp	42.4	58.11	*	0.72
C15	32	52.47	15.52	0.61
C30	28.58	52.81	18.6	0.54
C36	46.17	39.91	13.92	1.16
C40	36.4	50.88	12.72	0.72

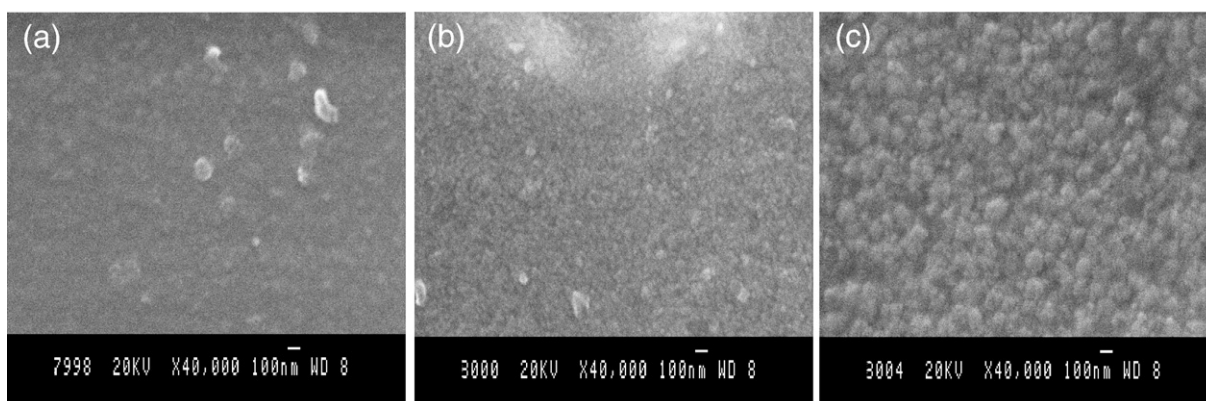


Fig. 2. (a) SEM micrographs of Cp, (b) SEM micrographs of C30 and (c) SEM micrographs of C40.

presence of a new cubic phase of  $\beta$ - $\text{In}_2\text{S}_3$  through the peak at  $2\theta = 28.8^\circ$ . Hence it became clear that the incorporation of chlorine slightly affected the tetragonal structure of  $\beta$ - $\text{In}_2\text{S}_3$  films.

### 3.1.2. EDAX measurements

Concentrations of In, S, and Cl in doped and pristine samples, obtained from EDAX analysis, are given in Table 2. As the concentration of sulfur in the spray solution was high, its atomic concentration in pristine film was almost that of the stoichiometric composition of 60%. It is reported that stoichiometric films were obtained from nitrate based samples prepared using a solution with higher sulfur concentration [26]. However as HCl concentration is increased, chlorine concentration in the films increased until the sample C30 and after that, it decreased. Also doping with Cl resulted in a decrease of the concentration of sulfur up to the sample C36. An increase in concentration of In from the sample C36 is also observed.

### 3.1.3. SEM and XPS analyses

Fig. 2(a), (b) and (c) exhibits the scanning electron micrographs of Cp, C30 and C40. Increase in grain size could be clearly observed, which supported the results obtained from the XRD analysis. It was also seen that the samples were free of pinholes and cracks.

XPS depth profile of the Cl doped sample (Fig. 3) showed the presence of chlorine at the surface and it is also clear that oxygen was present throughout the depth of the doped sample.

Thus the structural analysis proved that the Cl doping helped to form a crystallized compound in  $\beta$ - $\text{In}_2\text{S}_3$  structure. Decrease in sulfur concentration with Cl doping as seen from the EDAX measurements may be due to the incorporation of oxygen in Cl doped samples. Similar

nature of oxygen and sulfur was observed in  $\text{In}_2\text{S}_3$  films containing sodium [17].

## 3.2. Optical studies

### 3.2.1. Absorption studies

Optical absorption spectra were recorded in the wavelength region of 190–1200 nm. In order to determine the optical band gap,  $(\alpha h\nu)^2$  against  $h\nu$  graph was plotted (Fig. 4(a), (b) and (c)). Optical band gap was determined from this plot for all films by the linear fit in the straight portion of the graph. Band gap of the pristine sample was 2.74 eV. This value increased slightly with doped chlorine concentration and reached to 2.81 eV for the sample C36. This increase in band gap can be attributed to the incorporation of oxygen as sulfur concentration in films decreases. From EDAX, it is clear that sulfur concentration decreases up to the sample C36. XPS studies revealed incorporation of oxygen throughout the sample. Barreau et al. [17] reported an increase in band gap with oxygen concentration. But it could be seen that, on increasing the doping concentration above the optimum value, the band gap started decreasing. Band gap variation of the samples is evident from Table 3.

## 3.3. Electrical studies

### 3.3.1. Photosensitivity and resistivity

Hot probe measurements proved that all the films were *n*-type.

Photosensitivity (PS) measurements were performed and interestingly, it was observed that chlorine doping induced a drastic increase in photo response of the samples. Pristine sample has only a very low photosensitivity ( $\sim 15$ ) and maximum photosensitivity of 3 orders of

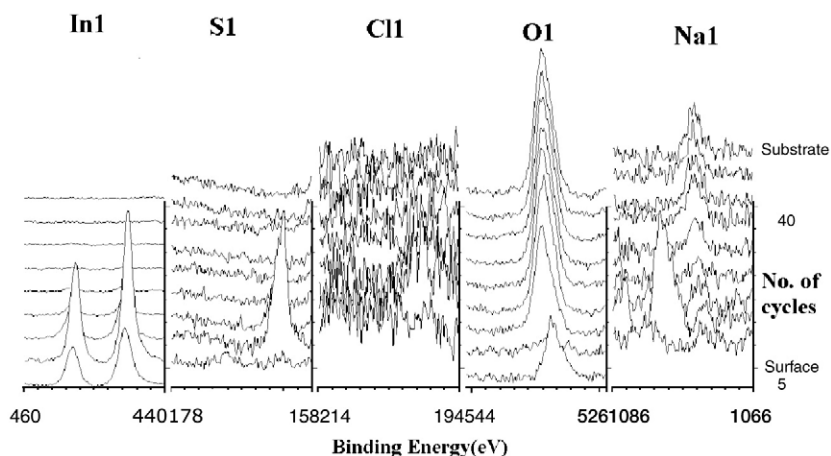


Fig. 3. XPS depth profile of C30 (no. of cycles means no. of etchings). The profile is from the surface of the sample (1st cycle) to the substrate (50th cycle).

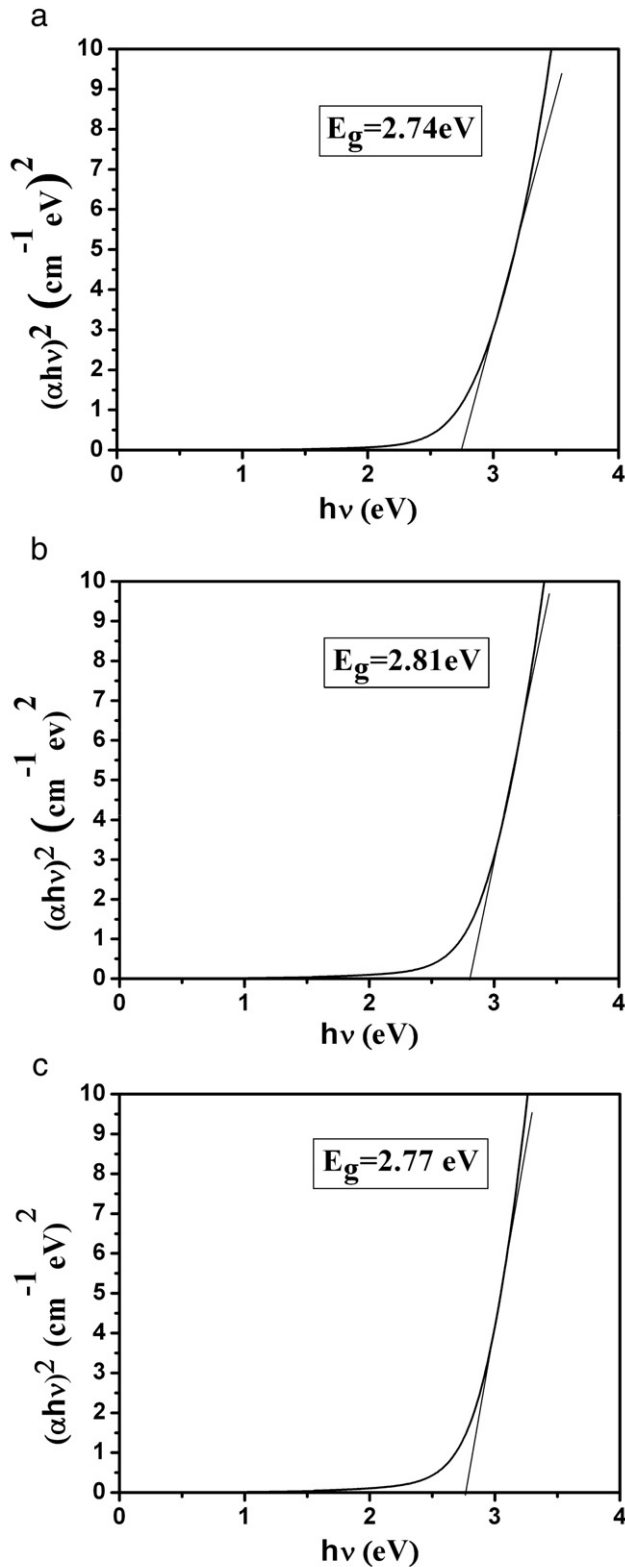


Fig. 4.  $(\alpha h\nu)^2$  vs  $h\nu$  plots of (a) Cp b) C36 and c) C40.

magnitude has been achieved for samples C30 and C36. C30 is the sample having a maximum Cl concentration in films as obtained from EDAX. For C36, Cl concentration in films started decreasing with an increase in concentration of indium. Therefore an increased concentration of Cl or In in the films is required for high photoresponse. Fig. 5(a) shows a graph plotted between photosensitivity ( $I_L - I_D/I_D$ ) and chlorine

**Table 3**  
Bandgap variation of pristine and chlorine doped samples.

Sample name	B.G.
Cp	2.74 eV
C15	2.74 eV
C30	2.78 eV
C36	2.81 eV
C40	2.77 eV

concentration.  $I_L$  is the current when the sample is illuminated with light and  $I_D$  is the dark current.

However, the resistivity also increased considerably from  $0.3 \Omega \text{ m}$  to  $550 \Omega \text{ m}$  with chlorine doping. Fig. 5(b) shows a graph plotted between resistivity and chlorine concentration.

Photosensitivity and resistivity values are tabulated in Table 4.

Increase in photosensitivity may be due to the increase in the minority carrier concentration in the valence band (VB) of this *n*-type material, without much recombination loss.

### 3.4. Conclusions

Doping  $\beta\text{-In}_2\text{S}_3$  thin films [prepared using CSP technique] with chlorine resulted in samples with higher photosensitivity and enhanced crystallinity. It was observed that there was an optimum amount of Cl so

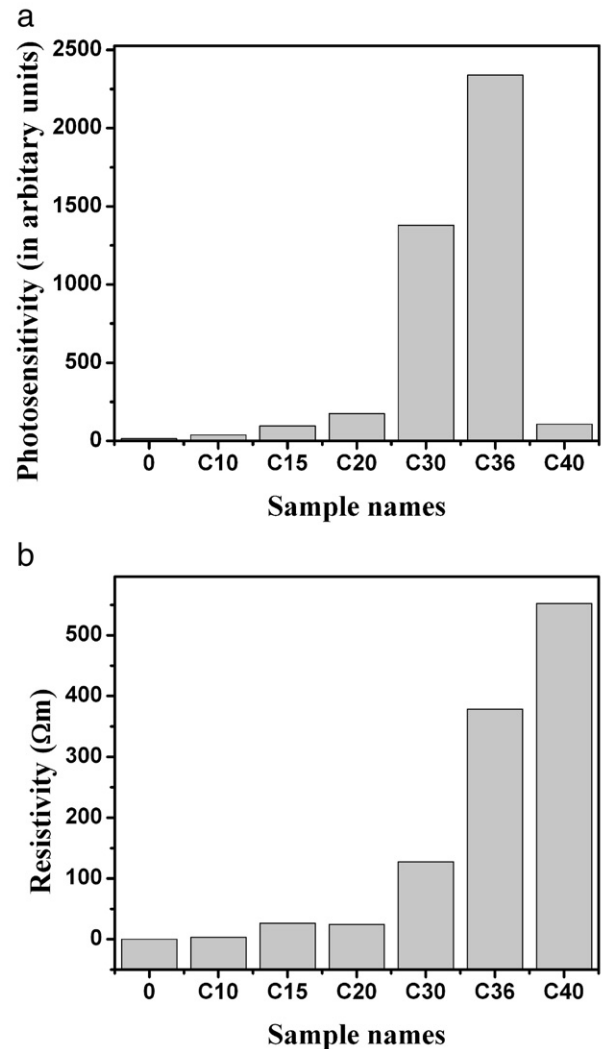


Fig. 5. (a) Photosensitivity vs sample names and (b) resistivity vs sample names.

**Table 4**  
Photosensitivity and resistivity variation of pristine and chlorine doped samples.

Sample	Photosensitivity	Resistivity( $\Omega$ m)
Cp	15.4	0.29
C10	38.66	3.2
C15	97.2	26.11
C20	175.1	24.3
C30	1379.1	127.1
C36	2339.1	378.5
C40	107.1	552.3

that further increase in doping concentration showed a decrease in the concentration of Cl in films. Photosensitivity has increased 3 orders of magnitude for the optimum Cl concentration (C30). Maximum photosensitivity is obtained for the sample C36, in which the Cl concentration in films started decreasing and In concentration in films started increasing. Therefore an increased concentration of In may also be a cause for high photoresponse. Also the electrical resistivity of the films increased drastically due to doping. Interestingly crystalline samples (C36) with high photosensitivity were also having higher band gap. This may be due to the incorporation of oxygen in films doped with Cl.

Thus it can be concluded that chlorine definitely plays a significant role in high photosensitivity of  $\beta$ -In<sub>2</sub>S<sub>3</sub> films, making the material useful for photovoltaic applications.

#### Acknowledgments

The authors would like to thank the Department of Science & Technology [DST] Government of India for providing the financial support [including fellowship] for this work. The facilities provided to our Department through the DSA-COSIST programme by the University Grants Commission were very useful for many of the analyses presented in this work. The authors gratefully acknowledge the whole hearted support of Prof. Y. Kashiwaba, Department of Electrical and Electronic Engineering, Iwate University, Japan for the XPS analysis.

#### References

- [1] O. Madelung, Data in Science and Technology: Semiconductors other than Group IV Elements and III–V Compounds, Springer-Verlag, Berlin-Heidelberg, 1992.
- [2] J.L. Vossen, W. Kern, Thin Films Processes, Academic Press, New York, NY, 1978.
- [3] P.K. Nair, M.T.S. Nair, V.M. Garcia, O.L. Arenas, Y. Peña, A. Castillo, I.T. Ayala, O. Gomez-Daza, A. Sanchez-Juarez, J. Campos, H. Hu, R. Suarez, M.E. Rincon, Sol. Energy Mater. Sol. Cells 52 (1998) 313.
- [4] P.M. Ratheesh Kumar, T.T. John, C. Sudha Kartha, K.P. Vijayakumar, T. Abe, Y. Kashiwaba, J. Mater. Sci. 41 (2006) 5519.
- [5] R.S. Becker, T. Zheng, J. Elton, M. Saeki, Sol. Energy Mater. 13 (1986) 97.
- [6] S. Yu, L. Shu, Y. Qian, Y. Xie, J. Yang, L. Yang, Mater. Res. Bull. 33 (1998) 717.
- [7] E. Dalas, L. Kobotiatis, J. Mater. Sci. 28 (1993) 6595.
- [8] K. Hara, K. Sayama, H. Arakawa, Sol. Energy Mater. Sol. Cells 62 (2000) 441.
- [9] N. Barreau, J.C. Bernede, S. Marsillac, C. Amory, W.N. Shafarman, Thin Solid Films 431–432 (2003) 326.
- [10] D. Braunger, D. Hariskos, T. Walthre, H.W. Schock, Sol. Energy Mater. Sol. Cells 40 (1996) 97.
- [11] T.T. John, M. Mathew, C. Sudha Kartha, K.P. Vijayakumar, T. Abe, Y. Kashiwaba, Sol. Energy Mater. Sol. Cells 89 (2005) 27.
- [12] R. Jayakrishnan, T. Theresa John, C. Sudha Kartha, K.P. Vijayakumar, T. Abe, Y. Kashiwaba, Semicond. Sci. Technol. 20 (2005) 1162.
- [13] W. Rehwald, G. Harbeke, J. Phys. Chem. Solids 26 (1965) 1309.
- [14] J.M. Giles, H. Hatwell, G. Offergeld, J. Van Cakenberghe, J. Phys. Stat. Sol. 2 (1962) K73.
- [15] R. Diehl, R. Nitsche, J. Cryst. Growth 28 (1975) 306.
- [16] K. Kambas, J. Spyridelis, M. Balkanski, Phys. Status Solidi B 105 (1981) 291.
- [17] N. Barreau, J.C. Bernede, C. Deudon, L. Brohan, S. Marsillac, J. Cryst. Growth 241 (2002) 4.
- [18] Mathew Meril, R. Jayakrishnan, P.M. Ratheesh Kumar, C. Sudha Kartha, Y. Kashiwaba, T. Abe, K.P. Vijayakumar, J. Appl. Phys. 100 (2006) 033504.
- [19] M. Rehwald, G. Harbeke, J. Phys. Chem. Solids 26 (1965) 1309.
- [20] John Teny Theresa, S. Bini, Y. Kashiwaba, T. Abe, Y. Yasuhiro, C. Sudha Kartha, K.P. Vijayakumar, Semicond. Sci. Technol. 18 (2003) 491.
- [21] P. O' Brien, D.J. Octway, J.R. Walsh, Thin Solid Films 315 (1998) 57.
- [22] M. Amlouk, M.A. Ben Said, N. Kamoun, S. Belgacem, N. Brunet, D. Barjon, Jpn. J. Appl. Phys. Part 1 38 (1999) 26.
- [23] R.S. Becker, T. Zheng, J. Elton, M. Saeki, Solar Energy Mater. 13 (1986) 97.
- [24] W.T. Kim, W.S. Lee, C.S. Chung, C.D. Kim, J. Appl. Phys. 63 (11) (1988) 5472.
- [25] N. Kamoun, S. Belgacem, M. Amlouk, R. Bennaceur, J. Bonnet, F. Touhari, M. Nouaoura, L. Lassabatere, J. Appl. Phys. 89 (5) (2001) 2766.
- [26] T.T. John, C. Sudha Kartha, K.P. Vijayakumar, T. Abe, Y. Kashiwaba, Appl. Surf. Sci. 252 (2005) 1360.
- [27] V. Consonni, G. Feuillet, S. Renet, J. Appl. Phys. 99 (2006) 053502.